

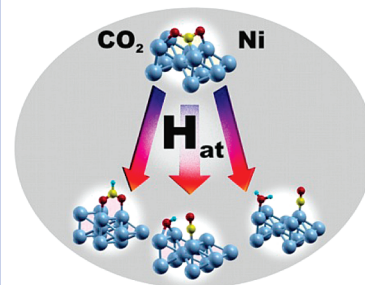
Hydrogen-Assisted Transformation of CO₂ on Nickel: The Role of Formate and Carbon Monoxide

Erik Vesselli,^{*,†} Michele Rizzi,^{‡,⊥} Loredana De Rogatis,^{◇,||} Xunlei Ding,^{§,∞} Alessandro Baraldi,[†] Giovanni Comelli,[†] Letizia Savio,[⊥] Luca Vattuone,^{⊥,⊗} Mario Rocca,^{⊥,⊗} Paolo Fornasiero,^{◇,▽} Alfonso Baldereschi,^{‡,#,⊥} and Maria Peressi^{‡,§}

[†]Physics Department and CENMAT, University of Trieste, Via A. Valerio 2, Trieste, Italy 34127, and Laboratorio Nazionale TASC INFN-CNR, Area Science Park SS 14 km 163.5, Basovizza (TS), Italy 34149, [◇]Chemistry Department, University of Trieste, Via L. Giorgieri 1, Trieste, Italy 34127, [▽]Italian Consortium on Materials Science and Technology (INSTM), [§]Theory@Elettra Group, DEMOCRITOS INFN-CNR National Simulation Center, Trieste, Italy, [⊥]DEMOCRITOS INFN-CNR National Simulation Center, Trieste, Italy, [‡]Theoretical Physics Department, University of Trieste, Strada Costiera 11, Trieste, Italy 34151, [#]Institute of Theoretical Physics, École Polytechnique Fédérale de Lausanne (EPFL), Lausanne, Switzerland 1015, [⊥]IMEM-CNR, Genova Operative Unit, and [⊗]Department of Physics, University of Genova, via Dodecanneso 33, Genova, Italy 16146

ABSTRACT The nanoscale description of the reaction pathways and of the role of the intermediate species involved in a chemical process is a crucial milestone for tailoring more active, stable, and cheaper catalysts, thus providing “reaction engineering” capabilities. This level of insight has not been achieved yet for the catalytic hydrogenation of CO₂ on Ni catalysts, a reaction of enormous environmental relevance. We present a thorough atomic-scale description of the mechanisms of this reaction, studied under controlled conditions on a model Ni catalyst, thus clarifying the long-standing debate on the actual reaction path followed by the reactants. Remarkably, formate, which is always observed under standard conditions, is found to be just a “dead-end” spectator molecule, formed via a Langmuir–Hinshelwood process, whereas the reaction proceeds through parallel Eley–Rideal channels, where hydrogen-assisted C–O bond cleavage in CO₂ yields CO already at liquid nitrogen temperature.

SECTION Surfaces, Interfaces, Catalysis



The catalytic conversion of CO₂ is a key chemical reaction, being the basis of photosynthesis in nature.¹ It has also been postulated that it had a role in the origin of life by synthesis of the first organic brick molecules, through the reaction with hydrogen or water, and catalyzed by metal particles in comet ice.² In industrial applications, CO₂ catalytic transformation for environmental, energetic, and organic synthesis is of primary relevance.^{3–6} To this purpose, due to the great chemical stability of CO₂, high Gibbs free-energy coreactants (like CH₄ or H₂)^{7,8} are required, together with metal catalysts able to activate the closed-shell molecule. The necessary progress in the design of innovative catalysts can be achieved by a deeper knowledge of the reaction mechanisms at the atomic scale, moving thus from the so-called trial-and-error approach widespread in catalysis research toward an engineered design.^{9,10} In the present paper, we clarify the long-standing debate existing in the literature about the actual reaction path followed by the reactants upon CO₂ hydrogenation on Ni, a widely used synthesis reaction. We prove that formate (HCOO), which is observed under standard conditions, is just a “dead-end” spectator and that the reaction proceeds via a hydrogen-assisted C–O bond cleavage in CO₂, yielding CO already at liquid nitrogen temperature.

This novel piece of information is of crucial importance for assessing the role of the intermediate species and the nature of the reactive sites in reactions involving CO₂ hydrogenation. These include a number of important industrial processes such as the Sabatier, Bosch, and reverse water gas shift reactions and methanol synthesis.^{5,11} In this respect, several aspects are unclear at present, such as for the Fischer–Tropsch reaction (CO + H₂) on Ni, where the role of CO is still under debate.¹¹ In this case, Ni is less active and selective toward CH₄ synthesis (chain lengthening occurs) than in the Sabatier reaction (CO₂ + H₂). The origin of this catalytic behavior remains unexplained and has tentatively been ascribed either to different reaction mechanisms or to different reactive surface species.^{11–13} A specific unsolved issue is the role of formate, which is detected as a stable species during CO₂ hydrogenation on Ni single-crystal or supported model catalysts.^{12,14–16} The following questions, in particular, have attracted general attention: (i) does formate react with H on nickel, (ii) is CO a reactive intermediate, and (iii) does CO stem from formate decomposition?¹² In order to answer

Received Date: November 5, 2009

Accepted Date: November 25, 2009

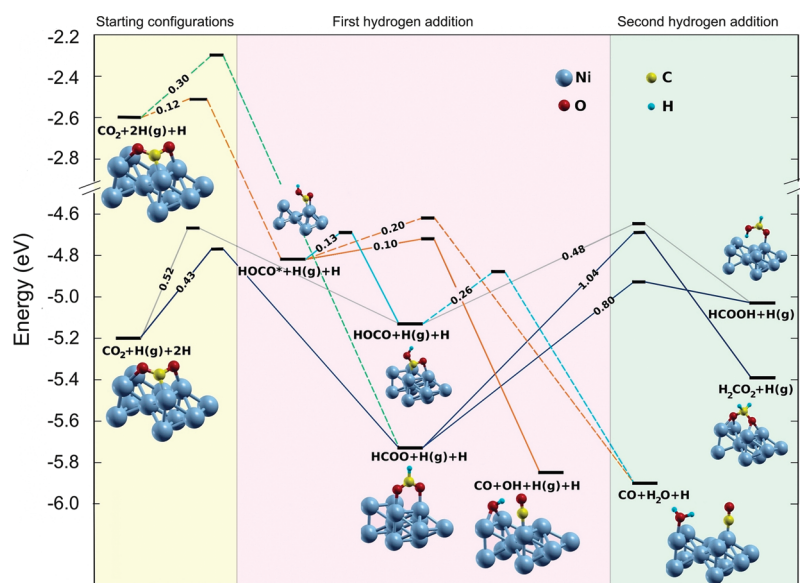


Figure 1. Energy diagram obtained by DFT calculations. Different possible CO_2 hydrogenation pathways on Ni(110) are indicated with solid and dashed lines for LH and ER mechanisms, respectively. Colors indicate different reaction pathways according to the text. Energies are given with respect to gas-phase (g) atomic H and chemisorbed CO_2 . In the ball-and-stick models of the relevant reactants, intermediates, and products, only Ni atoms of the outer layers are shown, but a five-layer-thick slab has been used in the calculations. HOCO^* indicates the “hot” hydrocarboxyl intermediate (see text for details).

these questions, an atomic-level insight into the complex reaction pathways is required.^{9,10} This can be achieved for a simplified model system by combining experimental and theoretical techniques. Following this approach, we demonstrate that under UHV conditions, HCOO^* is a “dead-end” product in a Langmuir–Hinshelwood (LH) hydrogenation reaction scheme on Ni(110). The (110) termination was chosen because CO_2 chemisorbs in a stable configuration under UHV on this surface, in contrast with other low-index single-crystal terminations where only physisorption occurs. In addition, we show that the reaction proceeds via an Eley–Rideal (ER) CO_2 hydrogenation mechanism, with competing parallel reaction pathways for selective formation of CO and HCOO^* .

Formate: A “Dead End” in the Hydrogenation Process. It is known that at 90 K, CO_2 chemisorbs on Ni(110) in a “V” configuration with a significant charge transfer from the metal surface (0.9 e^-).^{17,18} After dissociative coadsorption of H_2 at 90 K, CO_2 is hydrogenated at 150 K to a stable formate intermediate via a LH mechanism.^{15,16} The transition state involves a flip of the $\text{H}-\text{CO}_2$ complex with a low (0.43 eV)¹⁶ activation barrier (Figure 1, blue path at the left). In the present study, we find that further hydrogenation of HCOO^* by coadsorption with hydrogen does not occur, while heating the surface above 305 K yields HCOO^* dehydrogenation. CO synthesis by direct formate decomposition is not observed. Accordingly, our DFT calculations predict a very high energy barrier ($>3\text{ eV}$) for such decomposition. In analogy to the $\text{HCOO}/\text{Cu}(111)$ system,^{19,20} a barrier of $\sim 1\text{ eV}$ is found for the C–H cleavage in $\text{HCOO}/\text{Ni}(110)$ (Figure 1, blue path from the center to the left), a process which competes with further LH hydrogenation to dioxomethylene or to formic acid (Figure 1, blue paths from the center to the right). The latter, however,

Table 1. Calculated DFT Energies of the Relevant Reactants, Intermediates, And Products Participating in the CO_2 Hydrogenation on Ni(110) (same energy zero as in Figure 1)

reactants, intermediates and products	energy (eV)
$\text{CO}_2 + 2\text{H}(\text{g}) + \text{H}$	−2.60
$\text{CO}_2 + \text{H}(\text{g}) + 2\text{H}$	−5.20
$\text{HOCO}^* + \text{H}(\text{g}) + \text{H}$	−4.82
$\text{HOCO} + \text{H}(\text{g}) + \text{H}$	−5.13
$\text{HCOOH} + \text{H}(\text{g})$	−5.03
$\text{H}_2\text{CO}_2 + \text{H}(\text{g})$	−5.39
$\text{HCOO} + \text{H}(\text{g}) + \text{H}$	−5.73
$\text{CO} + \text{OH} + \text{H}(\text{g}) + \text{H}$	−5.85
$\text{CO} + \text{H}_2\text{O} + \text{H}$	−5.90

is unstable and decomposes back to formate. An alternative CO_2 hydrogenation path involves a different LH process (Figure 1, gray path). H reacts with an oxygen atom of the CO_2 molecule, overcoming a barrier of 0.52 eV (in close competition with CO_2 dissociation and desorption). This yields the formation of a reactive hydrocarboxyl intermediate, which can be subsequently hydrogenated to formic acid, followed finally by decomposition into formate. In conclusion, our results strongly indicate that under UHV, formate is very stable against further LH reaction with hydrogen and does not yield CO directly upon decomposition. In Table 1, we show the energies of the configurations reported in Figure 1.

A Parallel Route to CO. The reaction mechanism described above changes significantly when an atomic hydrogen beam is used.^{21,22} The 2.6 eV adsorption energy of H on Ni(110)¹⁶ is now partly available for the reaction, and new ER paths may open up. This, together with the adoption of molecular beams, is the approach normally used when working in UHV, in order

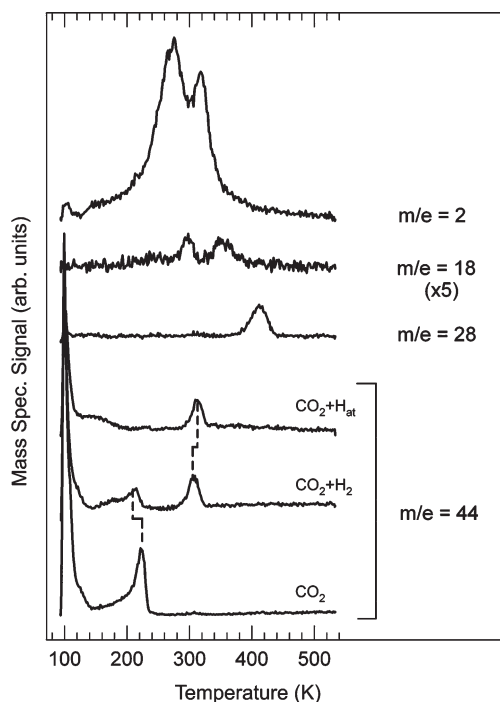


Figure 2. TPD spectra. Data are obtained after exposure of the $\text{CO}_2/\text{Ni}(110)$ layer (4 L) at 90 K to 10 L of atomic hydrogen; $m/e = 44$ spectra from the $\text{CO}_2/\text{Ni}(110)$ and the $\text{CO}_2 + \text{H}_2/\text{Ni}(110)$ layers are also shown for comparison (heating rate 1.5 K s^{-1}).

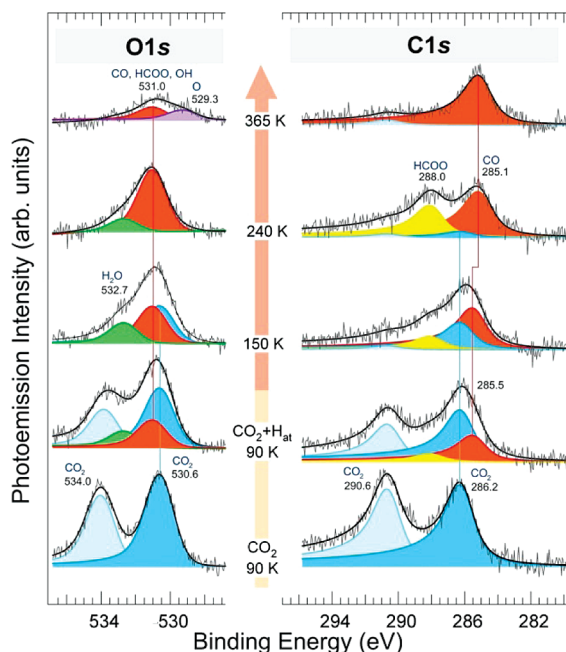


Figure 3. XPS spectra. O 1s (left panel) and C 1s (right panel) core-level spectra ($h\nu = 1253.6 \text{ eV}$) of the $\text{CO}_2/\text{Ni}(110)$ and $\text{CO}_2 + \text{H}_{\text{at}}/\text{Ni}(110)$ layers as a function of the annealing temperature; best fit curves and contributions as obtained by the fitting procedure are shown.

to compensate for the pressure gap, which yields a 0.6 eV lower chemical potential at room temperature.²³ Even though this approach does not guarantee direct transferability of UHV

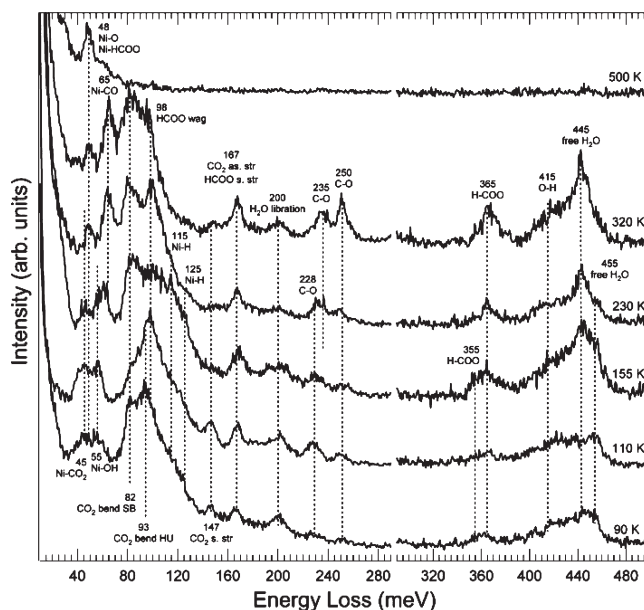


Figure 4. HREEL spectra of $\text{CO}_2 + \text{H}_{\text{at}}/\text{Ni}(110)$. Data were collected at 90 K after stepwise heating to selected temperatures (primary beam energy: 3.0 eV); in the C–H and O–H stretching region ($E > 290 \text{ meV}$), the curves have been magnified by a factor of five for clarity.

results to standard pressure conditions, it has been successfully used to investigate, at the atomic level, key steps of hydrogen-induced chemical reactions at surfaces in a controlled environment.²⁴ The latter is an essential condition to perform selective investigations on well-defined model systems, yielding results that can be used in direct comparison with theoretical descriptions.¹⁰

Following this approach, we expose a preadsorbed $\text{CO}_2/\text{Ni}(110)$ layer at 90 K (4 L,²⁵ 0.4 ML coverage²⁶) to gas-phase atomic hydrogen H_{at} (10 L). At this temperature, the most stable intermediates are frozen, while at higher temperature, they may be reactive and short-lived. Subsequent TPD experiments (Figure 2) indicate conversion of chemisorbed CO_2 into intermediate species which are stable up to 315 K and decompose into CO_2 , H_2 , and CO . Water production is also observed (295 and 350 K). Oxygen, strongly chemisorbed on Ni(110), is fairly reactive with hydrogen to yield water via a LH process in this temperature range under UHV conditions.^{27,28} This suggests that water is already formed at 90 K by direct H reaction with CO_2 and provides evidence for H-induced C–O bond cleavage in CO_2 .

After exposure to H_{at} at 90 K, the XPS spectra (Figure 3) show additional contributions at 288.0 and 285.5 eV (C 1s) and at 532.7 and 531.0 eV (O 1s) with respect to those of the pure CO_2 layer. The first three features are typical of HCOO ,¹⁶ a species containing a carbon atom bound to a single oxygen atom,¹⁶ and H_2O ,²⁷ respectively. The feature at 531.0 eV is compatible with the presence of CO , HCOO , and OH groups.^{16,27} XPS spectra therefore confirm the TPD hint that C–O bond scission in the CO_2 molecule has occurred already at 90 K. HREEL spectra at 90 K (Figure 4) show, in addition to the CO_2 losses,^{16,17} the presence of hydrogen (115, 125 meV),²⁹ formate (48, 98, 167, 355–365 meV),¹⁶ water

(200, 445, 455 meV),³⁰ and OH groups (55, 415 meV).³⁰ The losses at 228, 235, and 250 meV are ascribed to CO,³¹ which therefore forms already at 90 K upon a hydrogen-assisted CO₂ dissociation mechanism. The low intensity of the CO-related losses at 90 K is attributed both to the low CO coverage (0.10 ML) and to the screening effect due to the large overall coverage (~1 ML). TPD, XPS, and HREELS (Figures 2–4, respectively) spectra indicate that the CO coordination changes and its coverage increases upon annealing above 150 K. The C 1s core level shifts from 285.5 to 285.1 eV, consistent with previous core-level data for CO on Ni surfaces³² and in agreement with our DFT core-level calculations, which predict a 0.4 eV shift upon moving CO from the on-top to the bridge site. In parallel, LH processes yield formate (in competition with CO₂ decomposition), followed by HCOO dissociation and H₂, CO₂, H₂O, and CO desorption. A small residue of atomic oxygen is still present on the surface at 500 K.

A thorough analysis of the CO₂ + H ER reaction network on Ni(110) based on ab initio DFT results yields a straightforward interpretation of the experimental data. Indeed, we find an ER reaction channel yielding very stable coadsorbed CO and OH or water via a hydrocarboxyl precursor (Figure 1, orange path), whose activation barrier is as low as 0.12 eV. Alternatively, the hydrocarboxyl precursor can evolve into a more stable HOCO configuration, leading to CO and H₂O (cyan path). A competing path, with a 0.30 eV barrier for the first CO₂ ER hydrogenation, directly produces formate (green path). The energy barriers given above are small with respect to the kinetic energy that the impinging H atoms gain due to the attractive potential well of the metal surface. In particular, the first ER reaction step is thus easily accessible already at liquid nitrogen temperature.³³

We therefore provide direct theoretical and experimental evidence for a counterintuitive hydrogen-assisted CO₂ activation mechanism yielding C–O bond cleavage on Ni. This occurs via a hydrocarboxyl intermediate, similar to the path suggested with the support of DFT and microkinetic modeling for the reverse water gas shift reaction on Pt catalysts.³⁴ The reaction may be favored by those H atoms which do not react immediately with CO₂ and are trapped by the Ni surface underneath. After dissipating part of their energy, they react in a “hot” state with coadsorbed molecules. “Hot” intermediates can be generated,³³ thus favoring the reaction as in the case of the evolution of the hydrocarboxyl species (HOCO*, Figure 1). This picture is supported by the existing evidence³³ that, at most, 50% of the available energy is dissipated in similar systems in LH chemical reactions at metal surfaces, for example, by means of the creation of electron–hole pairs, and by the fact that this effect is even less pronounced in ER or “hot” atom reactions.

In this work, we have analyzed at the atomic scale the mechanisms of the CO₂ + H reaction network on Ni(110) under UHV conditions. In particular, we have demonstrated that (i) CO is an intermediate in the most favorable ER reaction paths, (ii) the adsorbed CO intermediate stems from ER hydrogenation of CO₂ at low temperature and not from formate, and (iii) in all reaction schemes, formate

is present and acts as a very stable spectator, with high and comparable LH reaction barriers for both dehydrogenation and further hydrogenation. By means of a combined theoretical and experimental approach, we have provided direct evidence for a hydrogen-assisted CO₂ activation mechanism yielding C–O bond cleavage via a carboxyl intermediate. The results provide insight into the CO₂ catalytic conversion reaction, offering (i) consistent and solid support to the previously proposed hypothesis that formate is not an intermediate of the CO₂ hydrogenation process and (ii) a detailed reaction mechanism which is compatible with all of the observations obtained under our working conditions. Direct transferability of our findings to standard conditions and supported catalysts is not straightforward due to the well-known pressure and material gaps. In this context, the use of the atomic hydrogen beam under UHV conditions has a specific relevance. Indeed, as discussed in the previous paragraphs, exposure of a surface to an atomic H beam determines in parallel the sampling of otherwise inaccessible ER reaction pathways and the creation of “hot”, reactive surface species. The latter mimic the high-energy and reactive H atoms emerging from the metal bulk interstitial absorption sites, which are populated, at variance with the UHV environment, under standard conditions, thus reducing the effective pressure gap.²⁴

Experimental and Computational Methods

We investigated the reaction mechanisms by combining UHV experimental findings obtained by temperature-programmed desorption (TPD), X-ray photoelectron spectroscopy (XPS),³⁵ and high-resolution electron energy loss spectroscopy (HREELS) with results based on ab initio density functional theory (DFT)³⁶ calculations. Geometries, energies, and core-level shifts have been calculated with the PWscf code of the Quantum ESPRESSO distribution³⁷ based on DFT. Reaction barriers have been evaluated by means of the nudged elastic band approach,³⁸ neglecting vibrational contributions. Details of all experimental and computational methods can be found in refs 17 and 18.

AUTHOR INFORMATION

Corresponding Author:

*To whom correspondence should be addressed. E-mail: Vesselli@tasc.infm.it. Phone: +39 040 375 6443. Fax: +39 040 226767.

Present Addresses:

^{||} University of Udine.

[∞] Chinese Academy of Science, Beijing.

ACKNOWLEDGMENT We acknowledge INFN-CNR for computational resources (Iniziativa trasversale di Calcolo Parallelo), UniTS (for the agreement with CINECA), Fondazione CRTrieste, Fondo Trieste, MIUR PRIN2007, Compagnia S. Paolo for financial support, and Osram SpA for technical support. We thank M. Kiskinova for fruitful discussions and C. T. Campbell, C. Dri, and K. C. Prince for reading the manuscript.

REFERENCES

- Barber, J. The Structure of Photosystem I. *Nat. Struct. Biol.* **2001**, *8*, 577–579.
- Bradley, J. P.; Brownlee, D. E.; Fraundorf, P. Carbon Compounds in Interplanetary Dust: Evidence for Formation by Heterogeneous Catalysis. *Science* **1984**, *223*, 56–58.
- Lackner, K. S. A Guide to CO₂ Sequestration. *Science* **2003**, *300*, 1677–1678.
- Sakakura, T.; Choi, J. C.; Yasuda, H. Transformation of Carbon Dioxide. *Chem. Rev.* **2007**, *107*, 2365–2387.
- Krylov, O. V.; Mamedov, A. K. Heterogeneous Catalytic Reactions of Carbon Dioxide. *Russ. Chem. Rev.* **1995**, *64*, 877–900.
- Varghese, O. K.; Paulose, M.; La Tempa, T. J.; Grimes, C. A. High-Rate Solar Photocatalytic Conversion of CO₂ and Water Vapor to Hydrocarbon Fuels. *Nano Lett.* **2009**, *9*, 731–737.
- Song, C. Global Challenges and Strategies for Control, Conversion and Utilization of CO₂ for Sustainable Development Involving Energy, Catalysis, Adsorption and Chemical Processing. *Catal. Today* **2006**, *115*, 2–32.
- Leitner, W. Carbon Dioxide as a Raw Material: The Synthesis of Formic Acid and its Derivatives from CO₂. *Angew. Chem., Int. Ed. Engl.* **1995**, *34*, 2207–2221.
- Nørskov, J. K.; Bligaard, T.; Kleis, J. Rate Control and Reaction Engineering. *Science* **2009**, *324*, 1655–1656.
- Nørskov, J. K.; Bligaard, T.; Rossmeisl, J.; Christensen, C. H. Towards the Computational Design of Solid Catalysts. *Nat. Chem.* **2009**, *1*, 37–46.
- Bundhoo, A.; Schweicher, J.; Frennet, A.; Kruse, N. Chemical Transient Kinetics Applied to CO Hydrogenation Over a Pure Nickel Catalyst. *J. Phys. Chem. C* **2009**, *113*, 10731–10739.
- Schild, C.; Wokaum, A.; Koepfel, R. A.; Baiker, A. CO₂ Hydrogenation Over Nickel/Zirconia Catalysts from Amorphous Precursors: the Mechanism of Methane Formation. *J. Phys. Chem.* **1991**, *95*, 6341–6346.
- Lapidus, A. L.; Gaidai, N. A.; Nekrasov, N. V.; Tishkova, L. A.; Agafonov, Yu. A.; Myshenkova, T. N. The Mechanism of Carbon Dioxide Hydrogenation on Copper and Nickel Catalysts. *Petr. Chem.* **2007**, *47*, 75–82.
- Nerlov, J.; Chorkendorff, I. Methanol Synthesis from CO₂, CO, and H₂ over Cu(100) and Ni/Cu(100). *J. Catal.* **1999**, *181*, 271–279.
- Freund, H.-J.; Roberts, M. W. Surface Chemistry of Carbon Dioxide. *Surf. Sci. Rep.* **1996**, *25*, 225–273.
- Vesselli, E.; De Rogatis, L.; Ding, X.; Baraldi, A.; Savio, L.; Vattuone, L.; Rocca, M.; Fornasiero, P.; Peressi, M.; Baldereschi, A.; et al. Carbon Dioxide Hydrogenation on Ni(110). *J. Am. Chem. Soc.* **2008**, *130*, 11417–11422.
- Ding, X.; De Rogatis, L.; Vesselli, E.; Baraldi, A.; Comelli, G.; Rosei, R.; Savio, L.; Vattuone, L.; Rocca, M.; Fornasiero, P.; et al. Interaction of Carbon Dioxide with Ni(110): A Combined Experimental and Theoretical Study. *Phys. Rev. B* **2007**, *76*, 195425.
- Ding, X.; Pagan, V.; Peressi, M.; Ancilotto, F. Modeling Adsorption of CO₂ on Ni(110) Surface. *Mater. Sci. Eng., C* **2007**, *27*, 1355–1359.
- Gokhale, A. A.; Dumesic, J. A.; Mavrikakis, M. On the Mechanism of Low-Temperature Water Gas Shift Reaction on Copper. *J. Am. Chem. Soc.* **2008**, *130*, 1402–1414.
- Mei, D.; Xu, L.; Henkelman, G. Dimer Saddle Point Searches to Determine the Reactivity of Formate on Cu(111). *J. Catal.* **2008**, *258*, 44–51.
- Bischler, U.; Bertel, E. Simple Source of Atomic Hydrogen for Ultrahigh Vacuum Applications. *J. Vac. Sci. Technol., A* **1993**, *11*, 458–460.
- Eibl, C.; Lackner, G.; Winkler, A. Quantitative Characterization of a Highly Effective Atomic Hydrogen Doser. *J. Vac. Sci. Technol., A* **1998**, *16*, 2979–2989.
- Hendriksen, B. L. M.; Bobaru, S. C.; Frenken, J. W. M. Looking at Heterogeneous Catalysis at Atmospheric Pressure Using Tunnel Vision. *Top. Catal.* **2005**, *36*, 43–54.
- Ceyer, S. T. The Unique Chemistry of Hydrogen Beneath the Surface: Catalytic Hydrogenation of Hydrocarbons. *Acc. Chem. Res.* **2001**, *34*, 737–744.
- 1 L = 1 × 10⁻⁶ torr·s.
- 1 ML is defined as 1 adsorbed atom or molecule per surface metal atom.
- Vesselli, E.; De Rogatis, L.; Baraldi, A.; Comelli, G.; Graziani, M.; Rosei, R. Structural and Kinetic Effects on a Simple Catalytic Reaction: Oxygen Reduction on Ni(110). *J. Chem. Phys.* **2005**, *122*, 144710.
- Sprunger, P. T.; Okawa, Y.; Besenbacher, F.; Stensgaard, I.; Tanaka, K. STM Investigation of the Coadsorption and Reaction of Oxygen and Hydrogen on Ni(110). *Surf. Sci.* **1995**, *344*, 98–110.
- Canning, N. D. S.; Chesters, M. A. The Co-Adsorption of H₂ and CO on Ni(110). *Surf. Sci.* **1986**, *175*, L811–L816.
- Hock, M. Coadsorption of Oxygen and Water at Ni(110). *Surf. Sci.* **1986**, *175*, L978–L982.
- Voigtländer, B.; Bruchmann, D.; Lehwald, S.; Ibach, H. Structure and Adsorbate–Adsorbate Interactions of the Compressed Ni(110)–(2 × 1)–CO Structure. *Surf. Sci.* **1990**, *225*, 151–161.
- Mårtensson, N.; Nilsson, A. In *Applications of Synchrotron Radiation*; Eberhardt, W., Ed.; Springer Series in Surface Science; Springer: Berlin, Germany, 1995; Vol. 35, p 65.
- Hasselbrink, E. Non-Adiabaticity in Surface Chemical Reactions. *Surf. Sci.* **2009**, *603*, 1564–1570.
- Grabow, L. C.; Gokhale, A. A.; Evans, S. T.; Dumesic, J. A.; Mavrikakis, M. Mechanism of the Water Gas Shift Reaction on Pt: First Principles, Experiments, and Microkinetic Modeling. *J. Phys. Chem. C* **2008**, *112*, 4608–4617.
- XPS peaks were fitted, after linear background subtraction, using Doniach–Šunjić line shapes convoluted with Gaussian profiles, see: Doniach, S.; Šunjić, M. *J. Phys. C* **1970**, *3*, 185.
- Jones, R. O.; Gunnarson, O. The Density Functional Formalism, its Applications and Prospects. *Rev. Mod. Phys.* **1989**, *61*, 689–746.
- Giannozzi, P.; Baroni, S.; Bonini, N.; Calandra, M.; Car, R.; Cavazzoni, C.; Ceresoli, D.; Chiarotti, G. L.; Cococcioni, M.; Dabo, I.; et al. QUANTUM ESPRESSO: a Modular and Open-Source Software Project for Quantum Simulations of Materials. *J. Phys.: Condens. Matter* **2009**, *21*, 395502.
- Jónsson, H.; Mills, G.; Jacobsen, K. W. In *Classical and Quantum Dynamics in Condensed Phase Simulations*; Berne, B. J., Ciccotti, G., Coker, D. F., Eds.; World Scientific: Singapore, 1998; p 385.